Report On

Analyzing Land Use Land Cover (LULC) Changes In IIT Kanpur Over 9 Years

The Report is submitted in fulfilment of the requirements

for the degree of M.tech in Geo informatics

by

Arka Dipta Sarkar, Ashis Aryal, Harsh Chandakar, Yuvraj Singh

Course Instructor

Dr. Bharat Lohani

DEPARTMENT OF CIVIL ENGINEERING

INDIAN INSTITUTE OF TECHNOLOGY KANPUR

November 2024

The aim of this project was to compute the land use and land cover changes of IIT Kanpur campus for a period of 9 years. Satellite imagery with at least a spatial resolution of 10 meters will be processed to classify the land into four principal categories: forest, open land, buildings, and roads. Using time-series analysis, we track changes in these types of land and produce a video or GIF that visually represents the transitions over time, giving an intuitive view of campus development and changes in environmental components. For higher reliability of the classifications, we produce accuracy matrices to test the precision of the categorization. We also analyze the trends found in LULC changes to understand the growth campus, impacts of urbanization, and transformation of the environment. Our research, therefore contributes to the establishment development understanding how land use from an institutional perspective has transformed institutions thus informing initiatives in sustainable management and campus planning. Various tools and datasets are used with further reference in the Appendix to guide your references.

Contents

Abstract **i**

List of Figures **iii**

1 Introduction **1**

2 Methodology **4**

3 Output and Discussion **12**

3.1 Output 13

3.2 Discussion 31

4 Conclusion **33**

Bibliography **34**

List of Figures

1.1 Study Area (IIT Kanpur campus) 3

2.1 Satellite Image Download 4
2.2 Study Are Clipping 5
2.3 Sample Training Tool 5
2.4 Training Sample Creation 6
2.5 Image Classification 6
2.6 Classified Image 7
2.7 Change Detection 7
2.8 Accuracy Assessment Points 8
2.9 Ground Truth Validation 8
2.10 Confusion matrix 9
2.11 Raster to Polygon 9
2.12 Display Polygon 10
2.13 Dissolve Polygon 10
2.14 Display Area Calculation 11

3.1 2016 Sentinel-2 image 13
3.2 2016 classified image 14
3.3 2016 confusion matrix 14
3.4 2017 Sentinel-2 image 15
3.5 2017 classified matrix 16
3.6 2017 confusion matrix 16
3.7 2018 Sentinel-2 image 17
3.8 2018 classified image 18
3.9 2018 confusion matrix 18
3.10 2019 Sentinel-2 image 19
3.11 2019 classified image 20
3.12 2019 confusion matrix 20
3.13 2020 Sentinel-2 image 21
3.14 2020 classified image 22
3.15 2020 confusion matrix 22
3.16 2021 Sentinel-2 image 23
3.18 2021 confusion matrix 24
3.17 2021 classified image 24

3.19 2022 Sentinel-2 image . . . 25
3.20 2022 classified image . . . 26
3.21 2022 confusion image . . . 26
3.22 2023 Sentinel-2 image . . . 27
3.23 2023 classified image . . . 28
3.24 2023 confusion matrix . . . 28
3.25 2024 Sentinel-2 image . . . 29
3.26 2024 classified image . . . 30
3.27 2024 confusion matrix . . . 30
3.28 Change Detection from 2016 to 2024 . . . 31

4.1 LULC change from 2016 to 2024 . . . 33

Chapter 1

Introduction

Land Use Land Cover (LULC) refers to the classification and mapping of land based on its observed physical and biological cover and its human usage. This classification often includes categories like forests, wetlands, urban areas, agricultural lands, and water bodies. LULC data is crucial for environmental monitoring, resource management, urban planning, and understanding environmental impacts.

Our project focuses on the Identification and characterization of LULC changes over the campus of IIT Kanpur over the last 9 years. This is a quantitative research using remote sensing data, coupled with the application of GIS techniques and advanced methods of classification that aims to quantify some changes in land use.

We have used ArcGIS Pro software and Sentinel 2A (L2A) image for carrying out this project. ArcGIS Pro is a comprehensive geographic information system (GIS) software developed by Esri. It's designed for visualizing, analyzing, and managing spatial data with advanced 2D and 3D mapping capabilities. Support Vector Machine algorithms have been used in this project for image classification. A Support Vector Machine (SVM) is a powerful supervised machine learning algorithm used for both classification and regression tasks, though it is primarily applied in classification. It can handle very large images and is less susceptible to noise, correlated bands, or an unbalanced number of training sites within each class.

Sentinel-2 L2A data is used for this project. L2A stands for Level 2A. The Sentinel 2 L2A imagery has undergone atmospheric correction, so it represents the Earth's surface reflectance, with atmospheric effects largely removed. The spatial resolution of the image was 10m. And dataset contains 8 layers.

One layer is for the red band which is stored in Band 4, another layer is for the green band which is stored in Band 3, another layer is for the blue band which is stored in Band 2. Similarly, another layer for the NIR band is stored in band 8. There are other four layers namely WVP, AOT, TCI, and Auxiliary Metadata File for TCI. Here, WVP stands for Water Vapor (WV) Product, AOT stands for Aerosol Optical Thickness (or Aerosol Optical Depth, AOD), and TCI stands for True Color Image. TCI data layer has been used in our project.

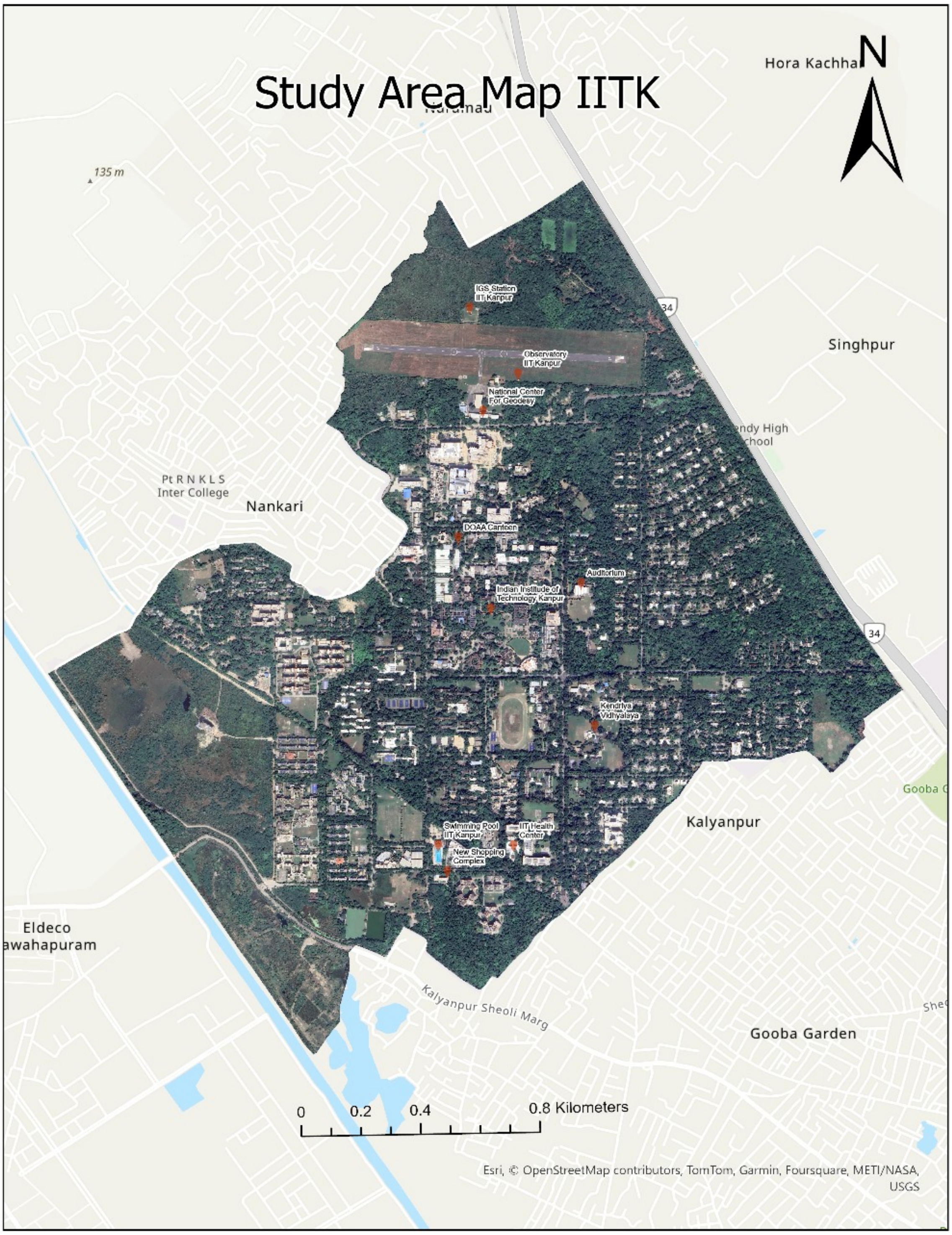

FIGURE 1.1: Study Area (IIT Kanpur campus)

Chapter 2

Methodology

- **Satellite Image Download**

  We began by downloading Sentinel-2 Level 2A (L2A) satellite imagery from the Copernicus Dataspace Ecosystem platform.

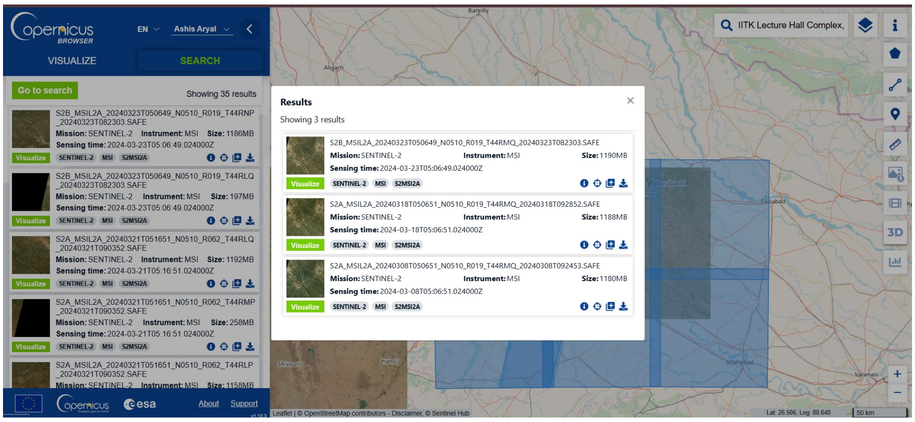

FIGURE 2.1: Satellite Image Download

- **Study Area Clipping**

  Using ArcGIS Pro, the TCI (True Color Image) layer from the downloaded dataset was clipped to focus specifically on our study area. This was achieved with the Extract by Mask tool.

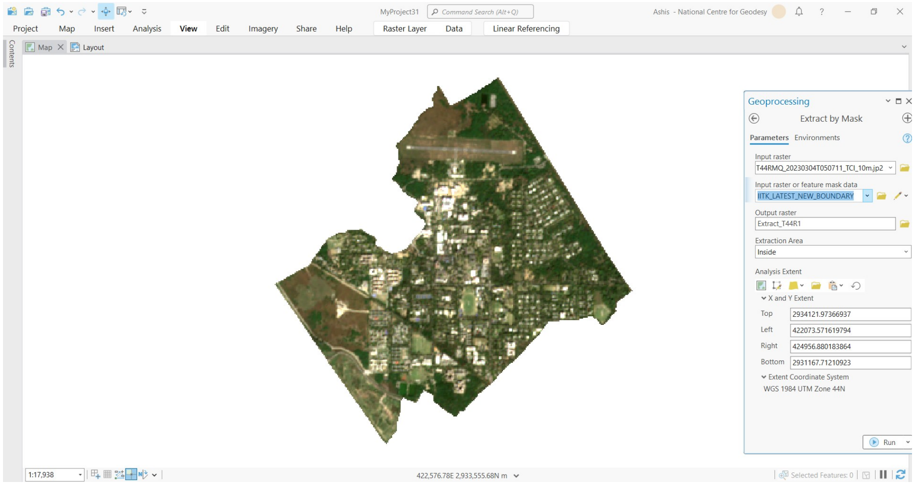

FIGURE 2.2: Study Are Clipping

- **Training Sample Creation**

  To classify the land cover, we used the Training Sample Manager under the Classification tools in the Imagery tab. We established a schema with four primary classes: Forest, Open Land, Building, and Road. Training pixels for each class were selected based on specific characteristics, such as pixel color, to ensure accurate classification.

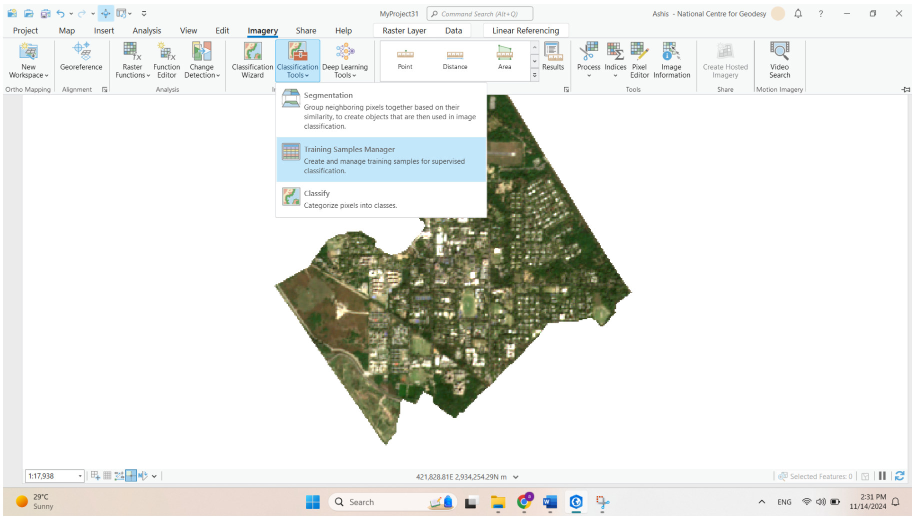

FIGURE 2.3: Sample Training Tool

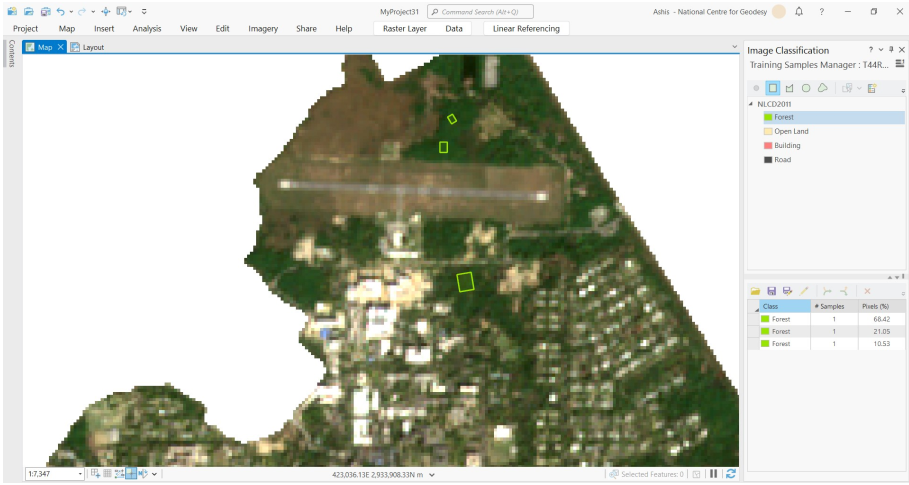

FIGURE 2.4: Training Sample Creation

- **Image Classification**

  The image classification was performed using the Support Vector Machine (SVM) Algorithm, which classified the imagery into the four specified classes based on our training samples. This classification process was repeated for nine images from different years (2016–2024), each representing the month of March to ensure seasonal consistency for accurate change analysis. All classified images for these years are shown below.

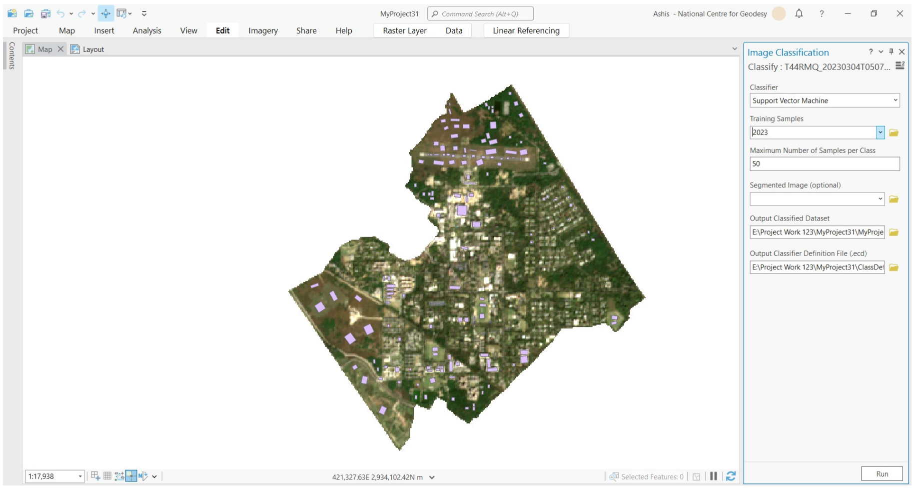

FIGURE 2.5: Image Classification

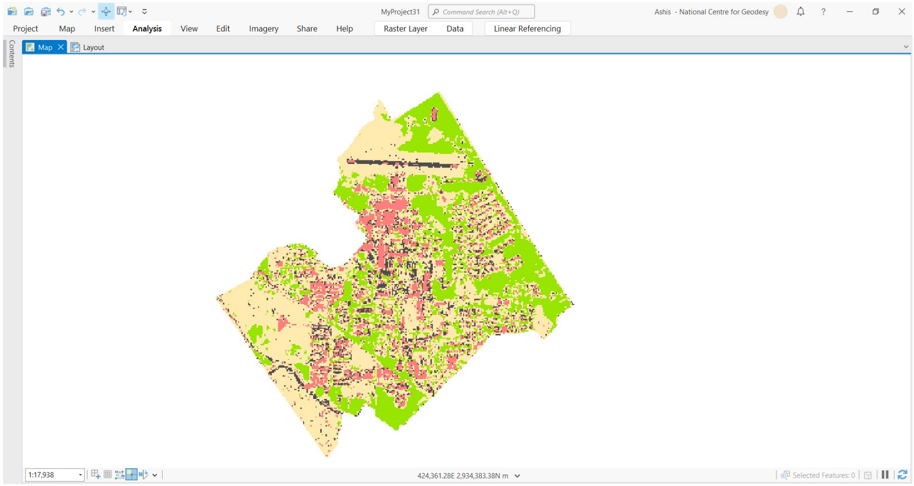

FIGURE 2.6: Classified Image

- **Change Detection Analysis**

  Using the Change Detection tool in the Imagery tab, we compared classified images from 2016 and 2024 to identify land cover changes over time. The results of this analysis are shown below.

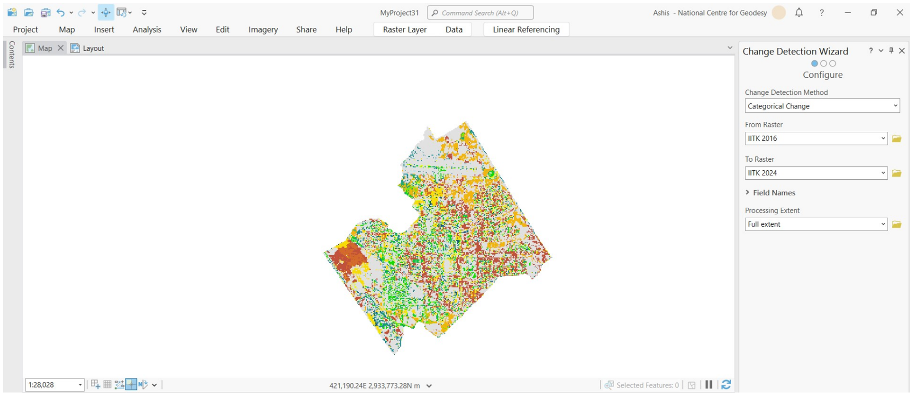

FIGURE 2.7: Change Detection

- **Accuracy Assessment**

  Accuracy assessment points were generated for each classified image using the Create Accuracy Assessment Point tool to build a confusion matrix. This matrix provides a quantitative assessment of the classification accuracy.

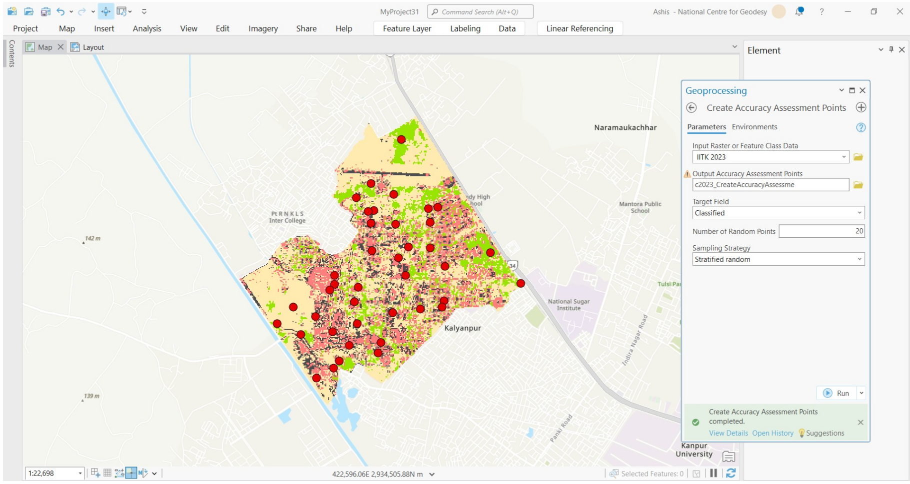

FIGURE 2.8: Accuracy Assessment Points

- **Ground Truth Validation**

  To validate the classification accuracy, Google Earth Pro images from the respective years were used as ground truth. Ground truth data were entered into the attribute table for each year.

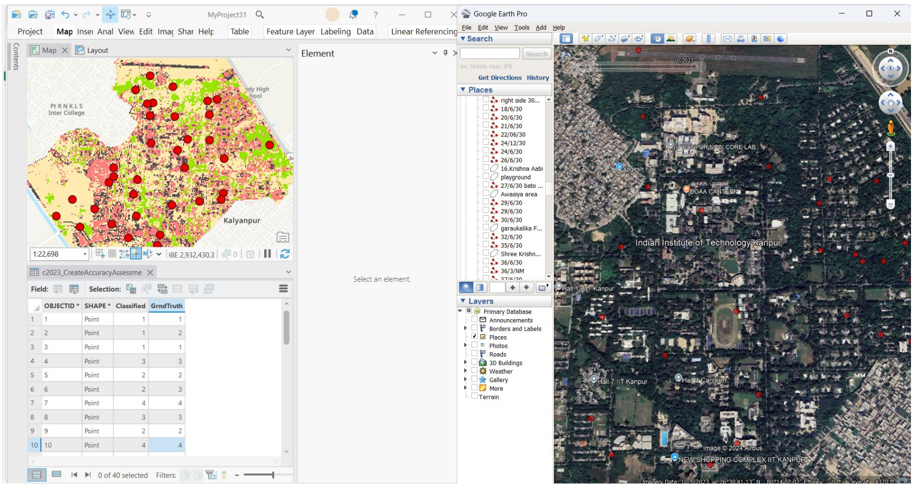

FIGURE 2.9: Ground Truth Validation

- **Confusion Matrix Analysis**

  The Compute Confusion Matrix tool was used to generate confusion matrices for each classified image. These matrices include measures such as user's accuracy, producer's accuracy, and the kappa index, which quantify the classification accuracy. The results are presented in a table below.

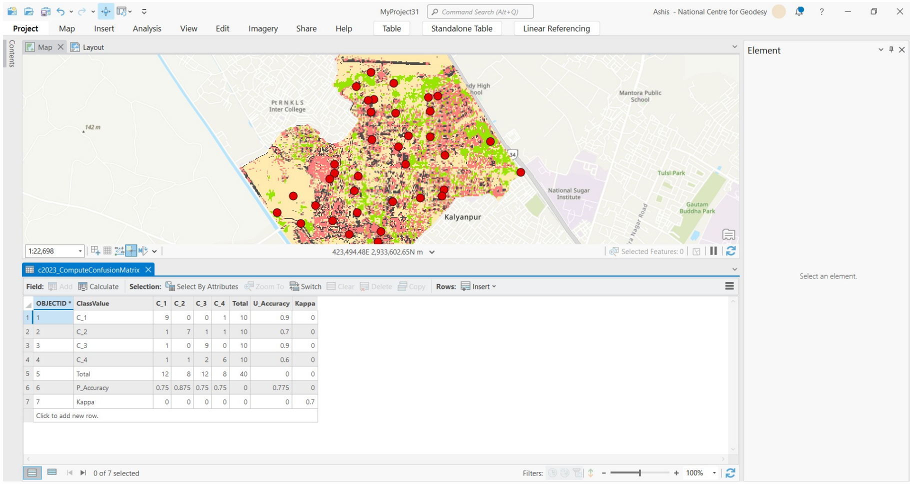

FIGURE 2.10: Confusion matrix

- **Area Calculation for Each Class**

  Finally, we calculated the area covered by each class for the years 2016 and 2024. This was done by converting the classified images to polygons using the Raster to Polygon tool, followed by dissolving the polygons based on class names. This provided the total area for each land cover class, which we visualized in a bar graph to show the changes in land use over time.

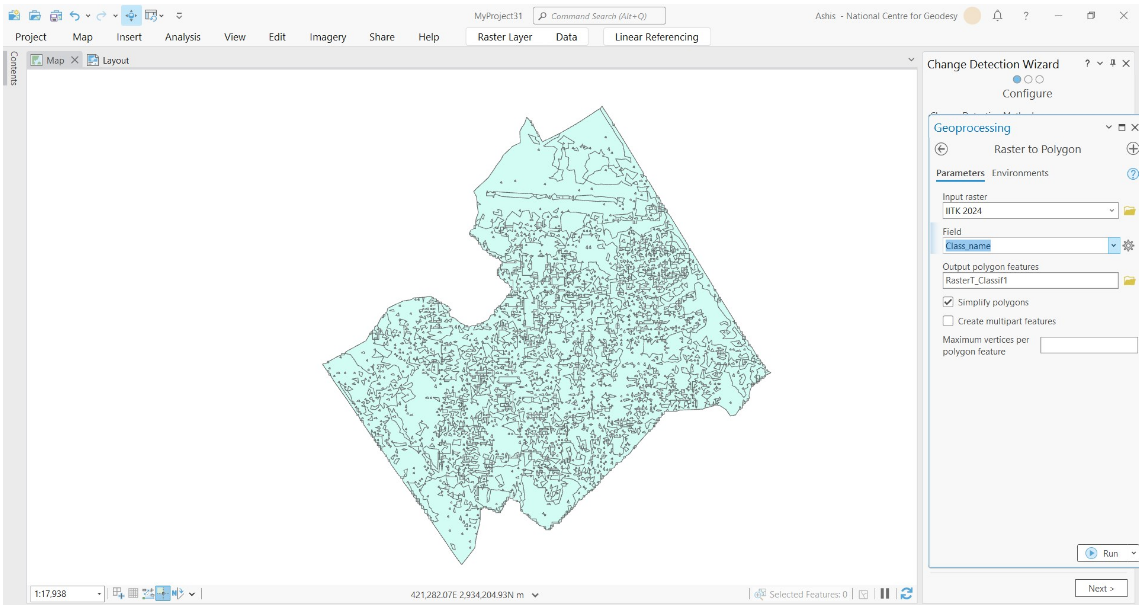

FIGURE 2.11: Raster to Polygon

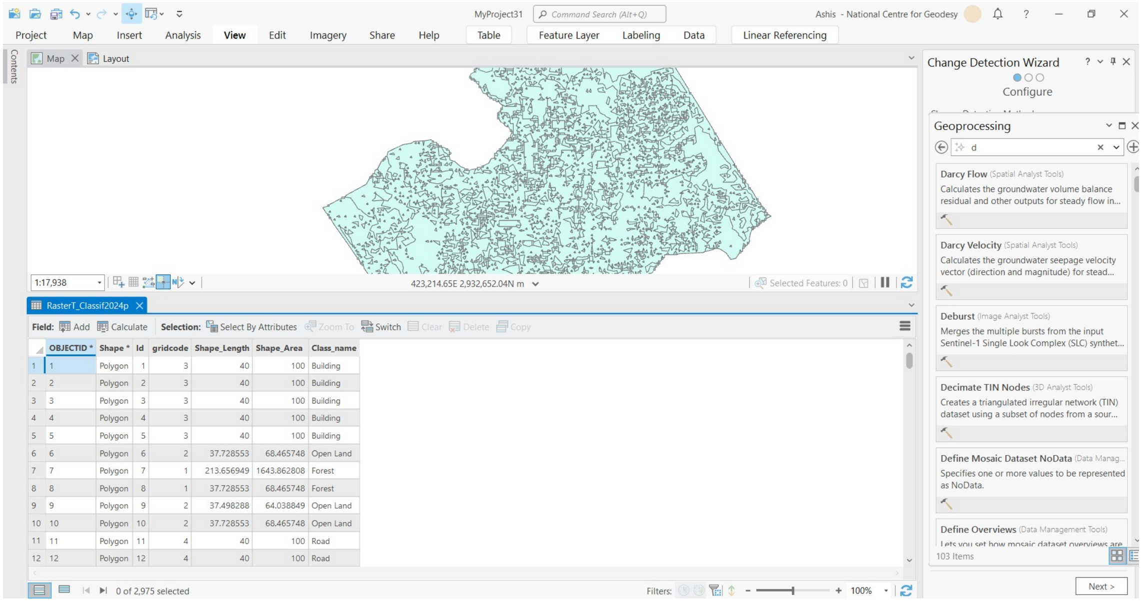

FIGURE 2.12: Display Polygon

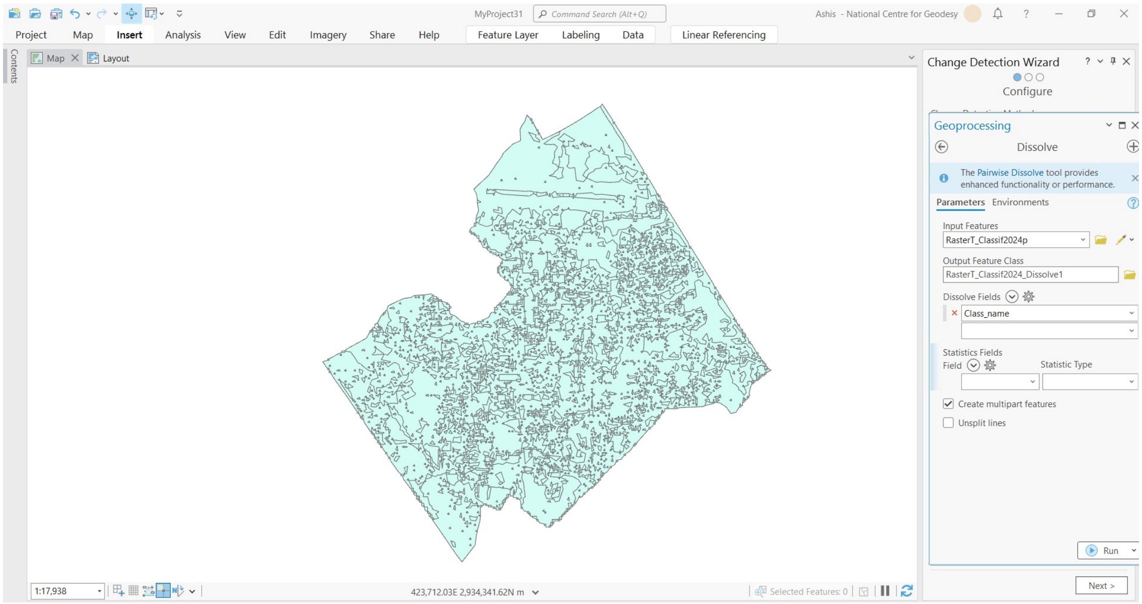

FIGURE 2.13: Dissolve Polygon

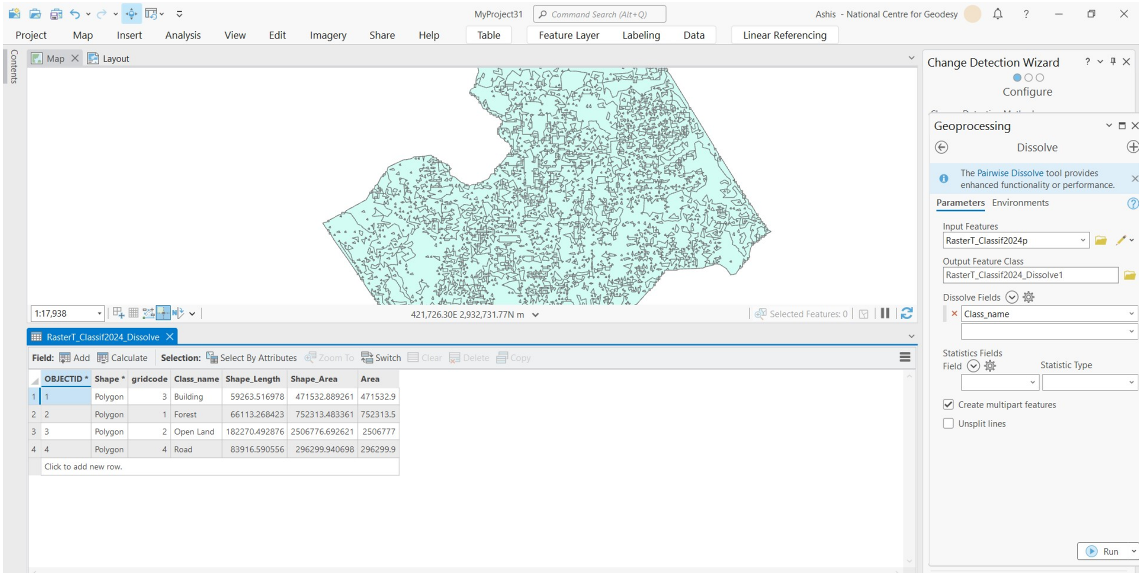

FIGURE 2.14: Display Area Calculation

Chapter 3

Output and Discussion

3.1 Output

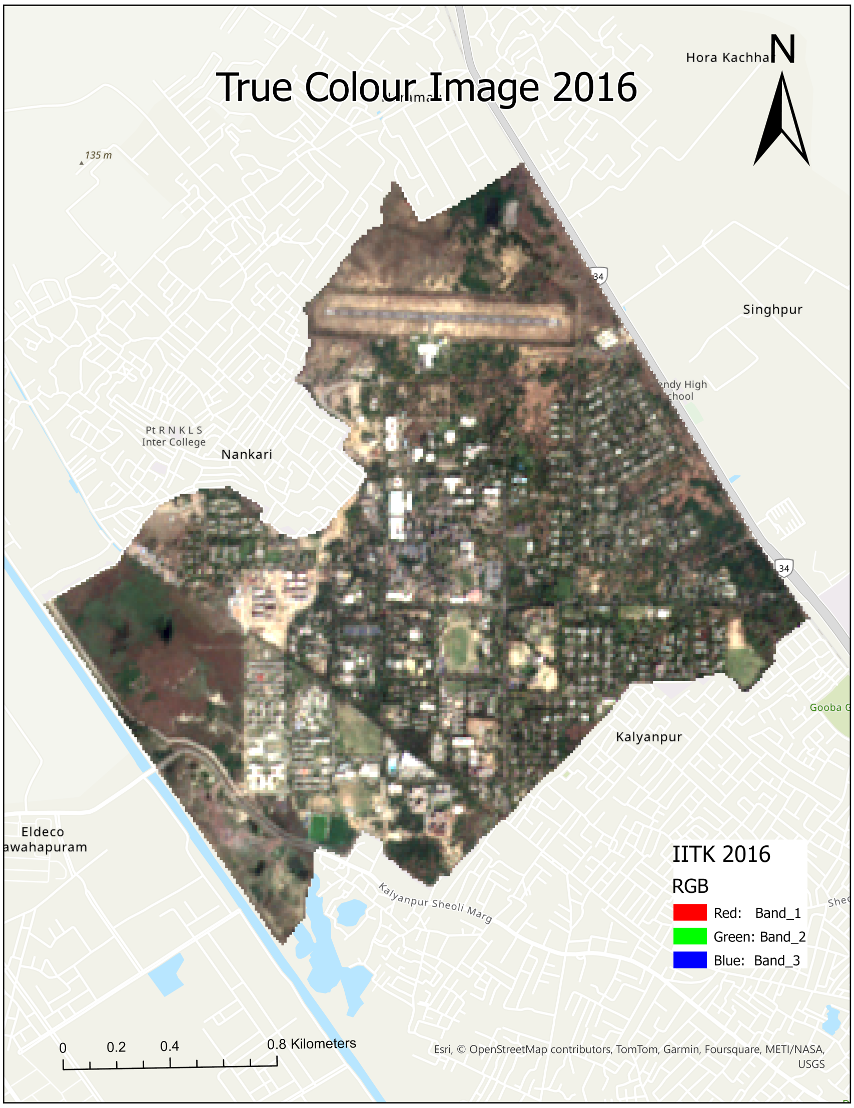

FIGURE 3.1: 2016 Sentinel-2 image

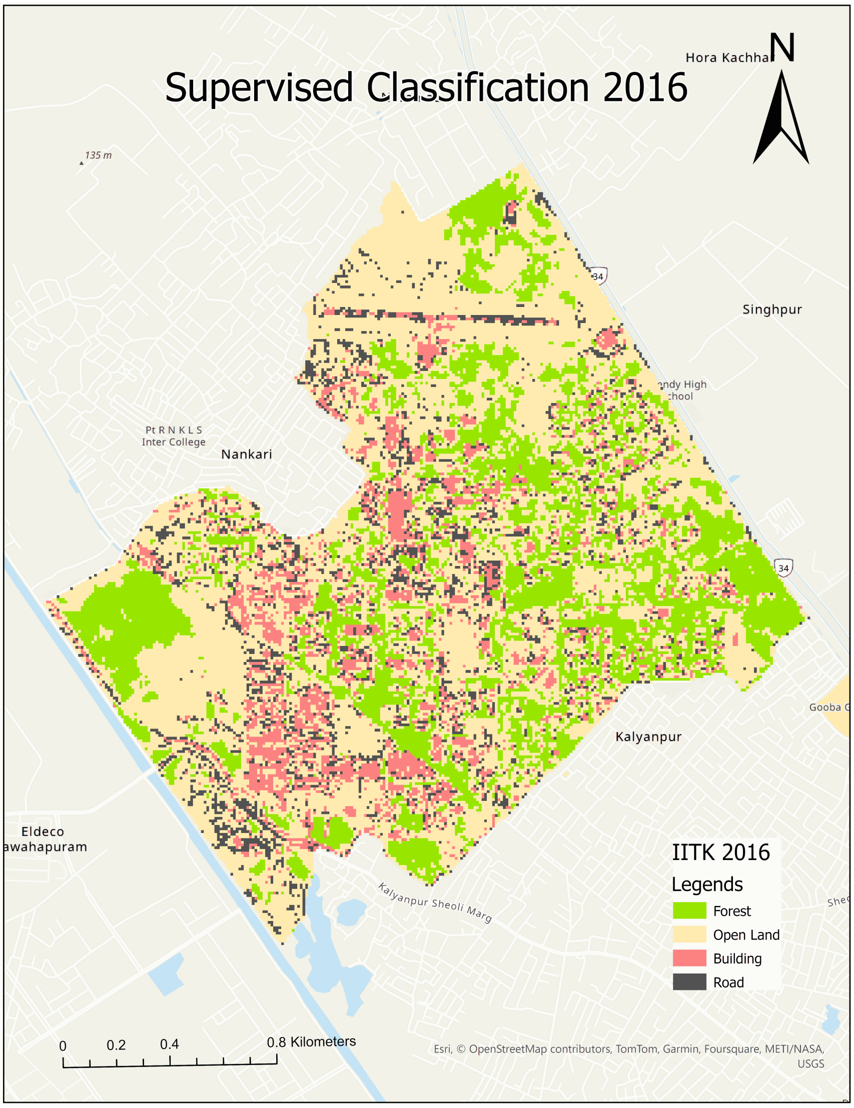

FIGURE 3.2: 2016 classified image

	OBJECTID *	ClassValue	C_1	C_2	C_3	C_4	Total	U_Accuracy	Kappa
1	1	C_1	10	0	0	0	10	1	0
2	2	C_2	0	10	0	1	11	0.909091	0
3	3	C_3	1	0	9	0	10	0.9	0
4	4	C_4	0	2	3	5	10	0.5	0
5	5	Total	11	12	12	6	41	0	0
6	6	P_Accuracy	0.909091	0.833333	0.75	0.833333	0	0.829268	0
7	7	Kappa	0	0	0	0	0	0	0.772041

FIGURE 3.3: 2016 confusion matrix

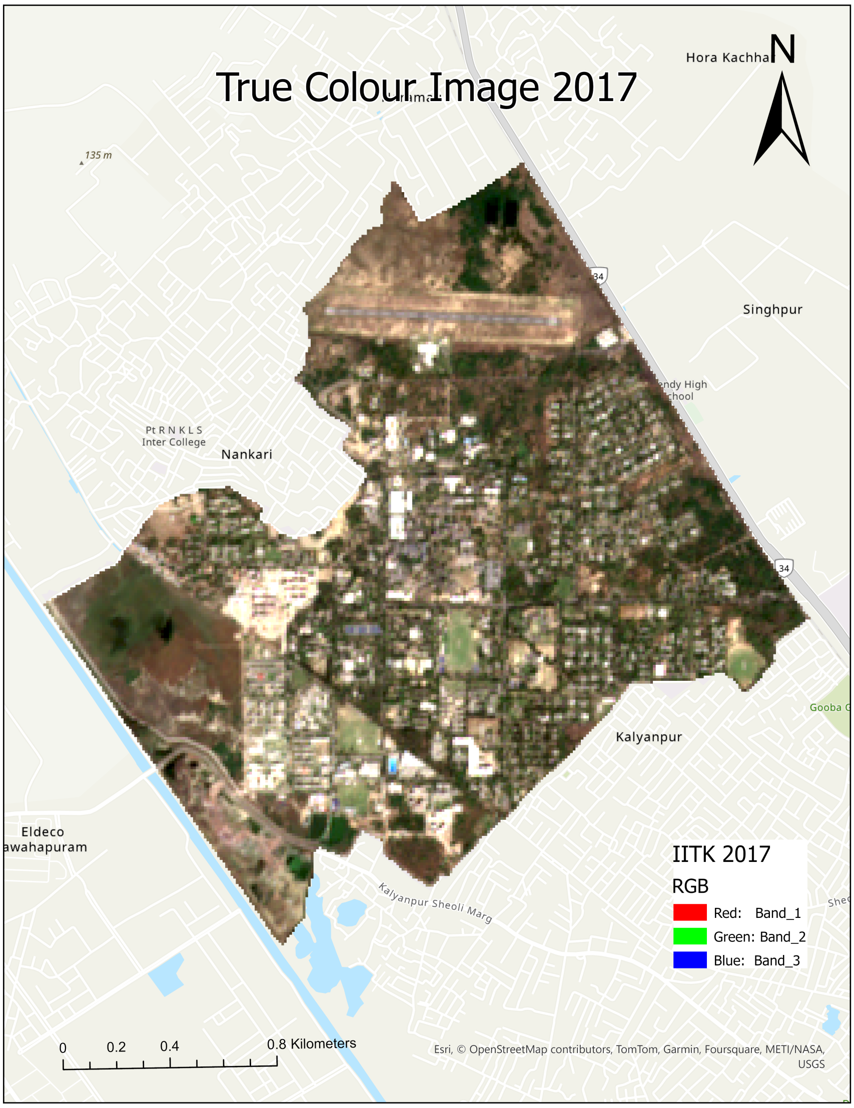

FIGURE 3.4: 2017 Sentinel-2 image

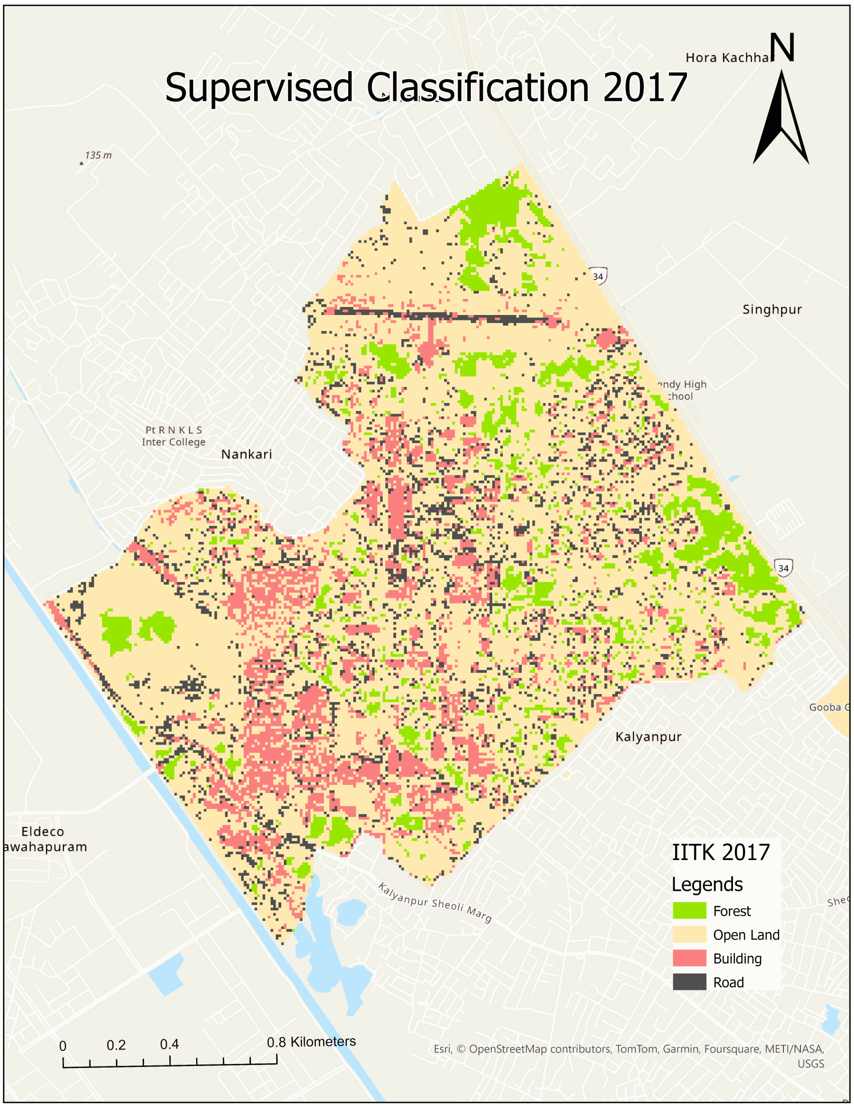

FIGURE 3.5: 2017 classified matrix

	OBJECTID *	ClassValue	C_1	C_2	C_3	C_4	Total	U_Accuracy	Kappa
1	1	C_1	10	0	0	0	10	1	0
2	2	C_2	0	13	0	0	13	1	0
3	3	C_3	0	2	7	1	10	0.7	0
4	4	C_4	0	3	1	6	10	0.6	0
5	5	Total	10	18	8	7	43	0	0
6	6	P_Accuracy	1	0.722222	0.875	0.857143	0	0.837209	0
7	7	Kappa	0	0	0	0	0	0	0.779487

FIGURE 3.6: 2017 confusion matrix

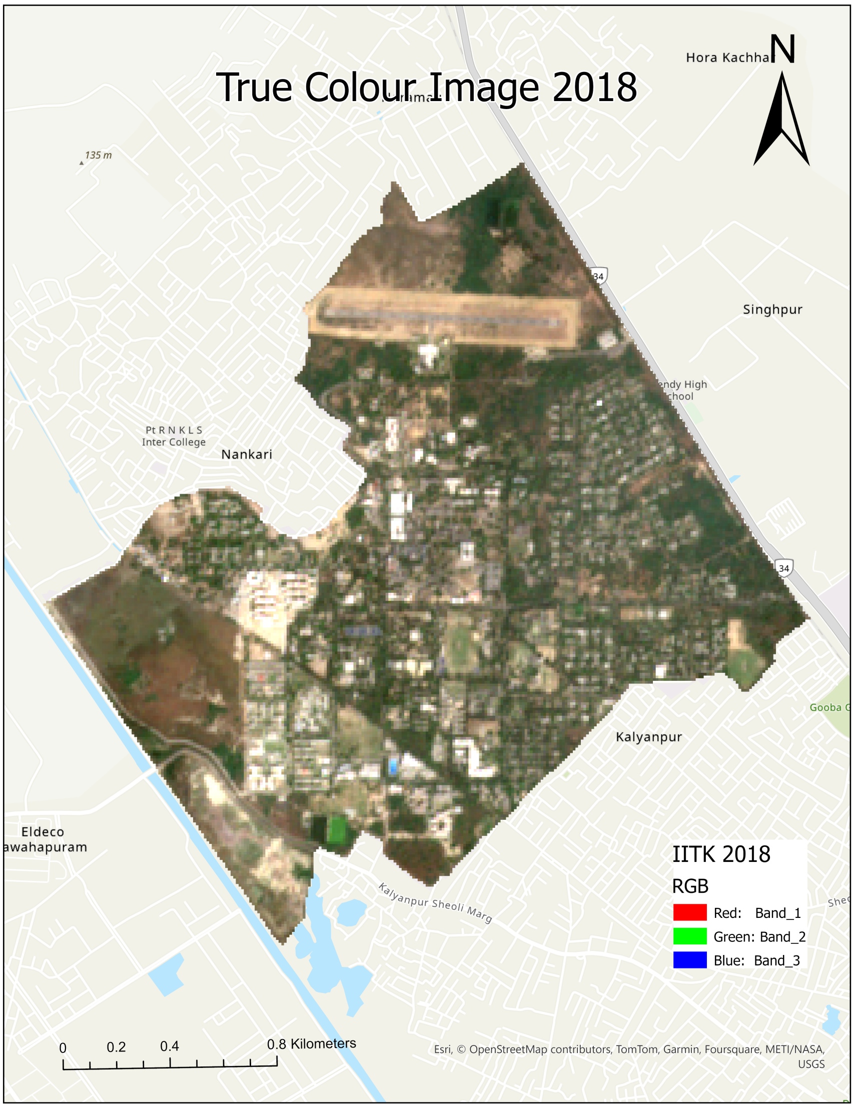

Figure 3.7: 2018 Sentinel-2 image

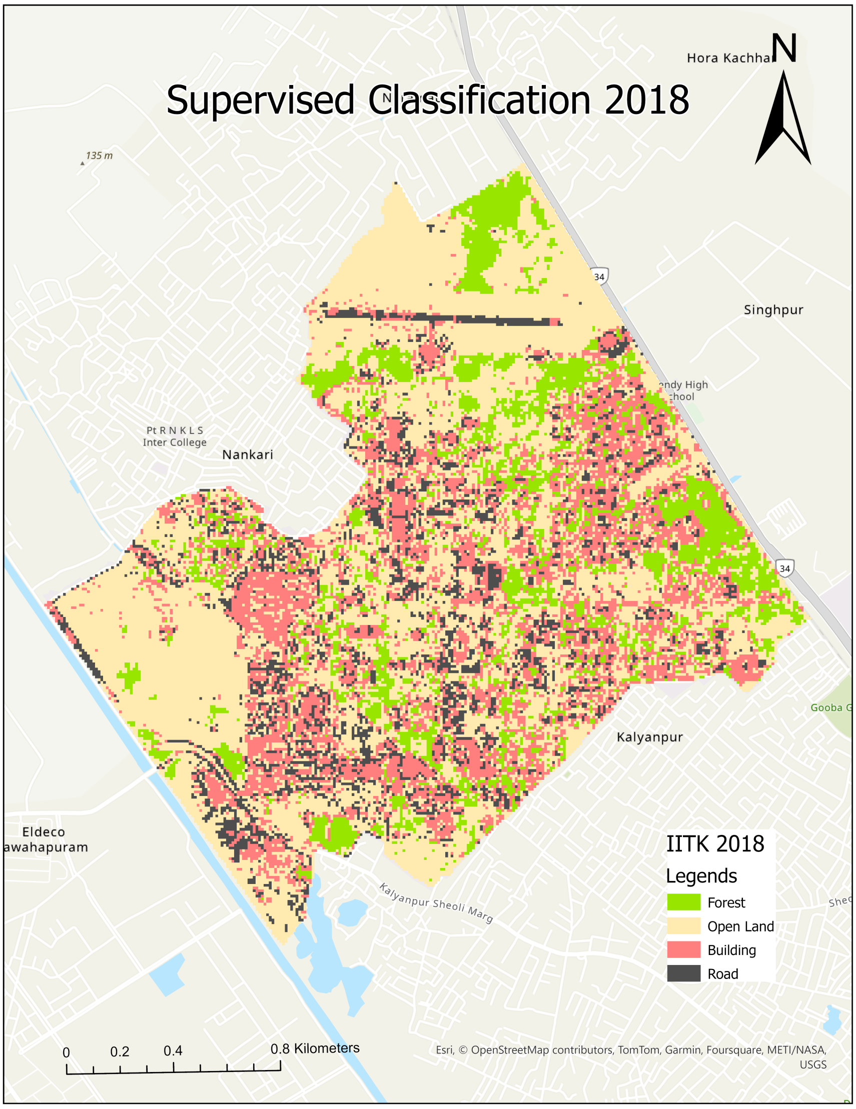

FIGURE 3.8: 2018 classified image

	OBJECTID *	ClassValue	C_1	C_2	C_3	C_4	Total	U_Accuracy	Kappa
1	1	C_1	10	0	0	0	10	1	0
2	2	C_2	0	10	0	0	10	1	0
3	3	C_3	1	0	8	0	9	0.888889	0
4	4	C_4	0	0	3	7	10	0.7	0
5	5	Total	11	10	11	7	39	0	0
6	6	P_Accuracy	0.909091	1	0.727273	1	0	0.897436	0
7	7	Kappa	0	0	0	0	0	0	0.863398

FIGURE 3.9: 2018 confusion matrix

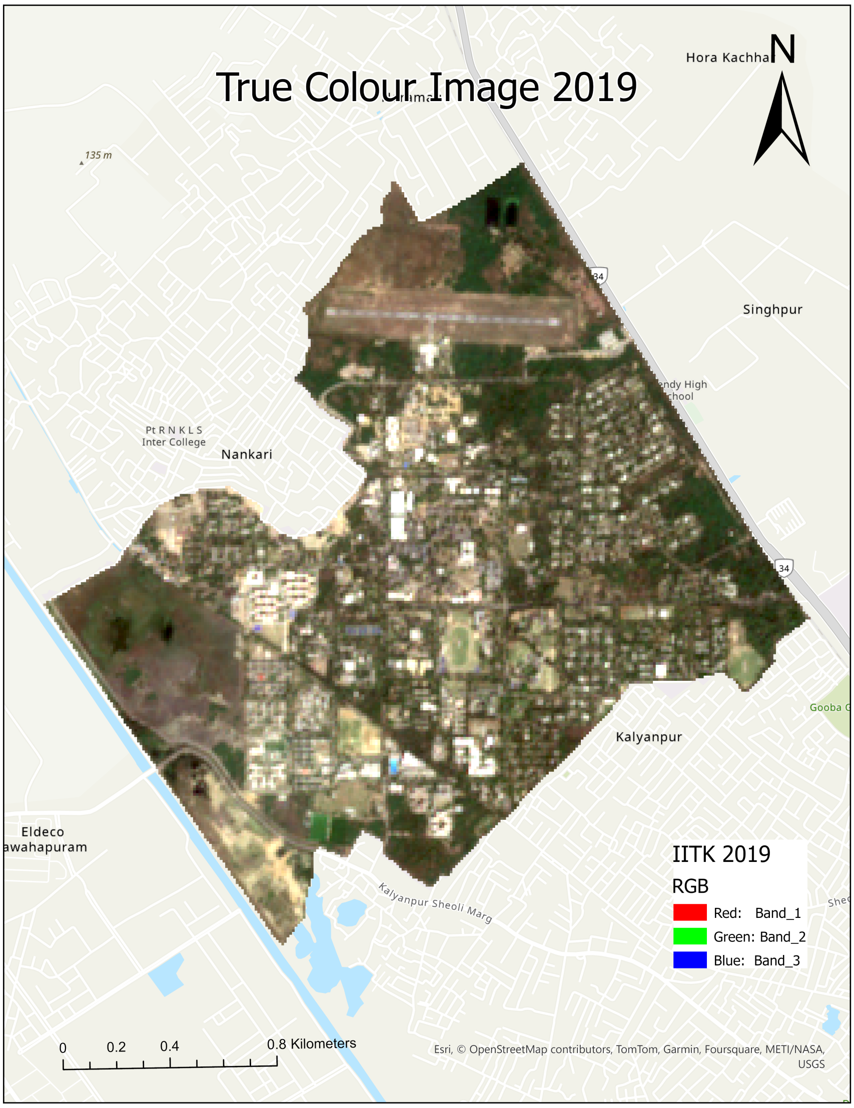

FIGURE 3.10: 2019 Sentinel-2 image

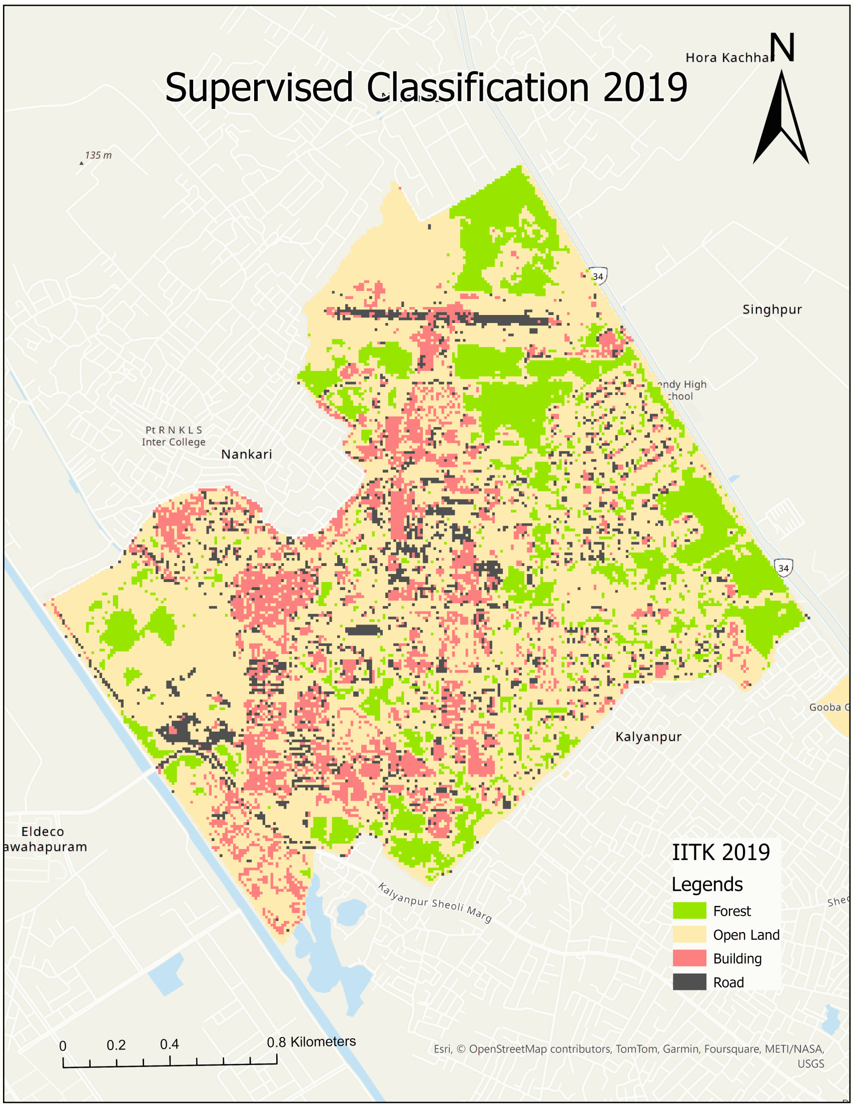

FIGURE 3.11: 2019 classified image

	OBJECTID *	ClassValue	C_1	C_2	C_3	C_4	Total	U_Accuracy	Kappa
1	1	C_1	6	1	0	0	7	0.857143	0
2	2	C_2	0	11	0	0	11	1	0
3	3	C_3	0	1	1	0	2	0.5	0
4	4	C_4	0	0	3	3	6	0.5	0
5	5	Total	6	13	4	3	26	0	0
6	6	P_Accuracy	1	0.846154	0.25	1	0	0.807692	0
7	7	Kappa	0	0	0	0	0	0	0.72043
	Click to add new row.								

FIGURE 3.12: 2019 confusion matrix

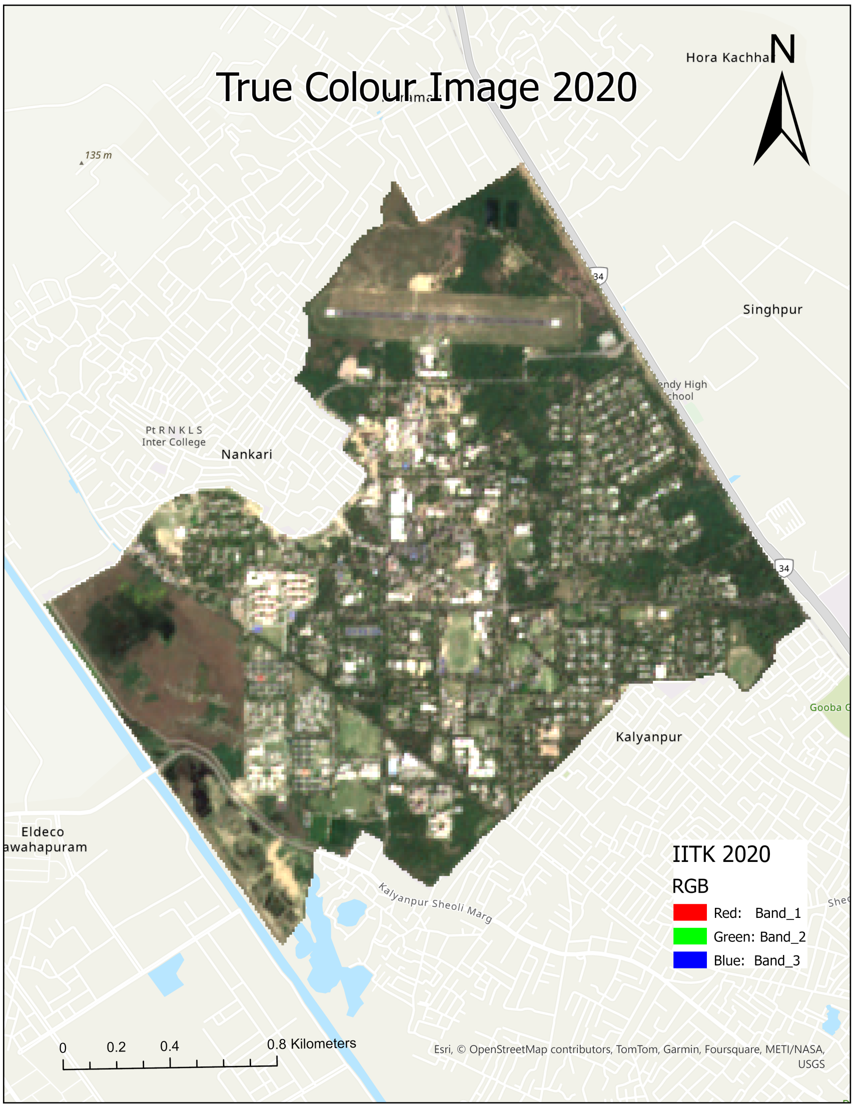

FIGURE 3.13: 2020 Sentinel-2 image

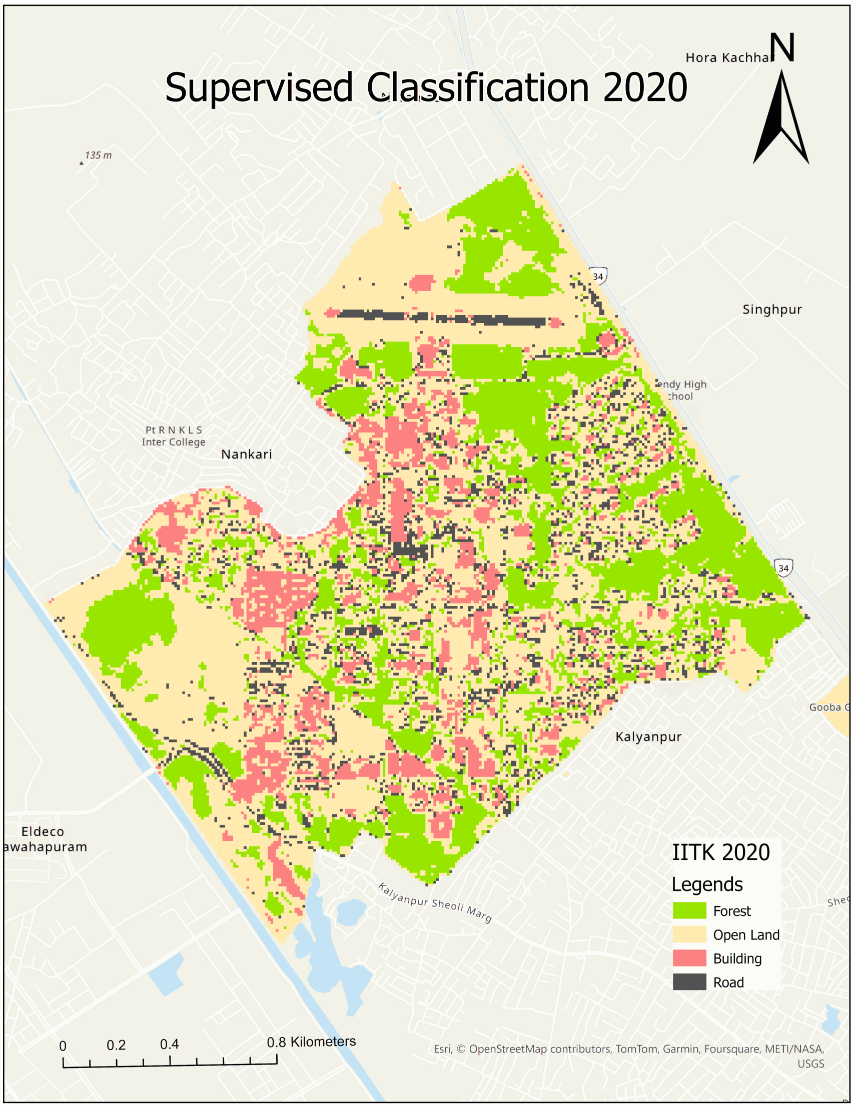

FIGURE 3.14: 2020 classified image

	OBJECTID *	ClassValue	C_1	C_2	C_3	C_4	Total	U_Accuracy	Kappa
1	1	C_1	6	0	0	0	6	1	0
2	2	C_2	0	7	0	0	7	1	0
3	3	C_3	0	1	2	1	4	0.5	0
4	4	C_4	0	0	2	6	8	0.75	0
5	5	Total	6	8	4	7	25	0	0
6	6	P_Accuracy	1	0.875	0.5	0.857143	0	0.84	0
7	7	Kappa	0	0	0	0	0	0	0.78308
	Click to add new row.								

FIGURE 3.15: 2020 confusion matrix

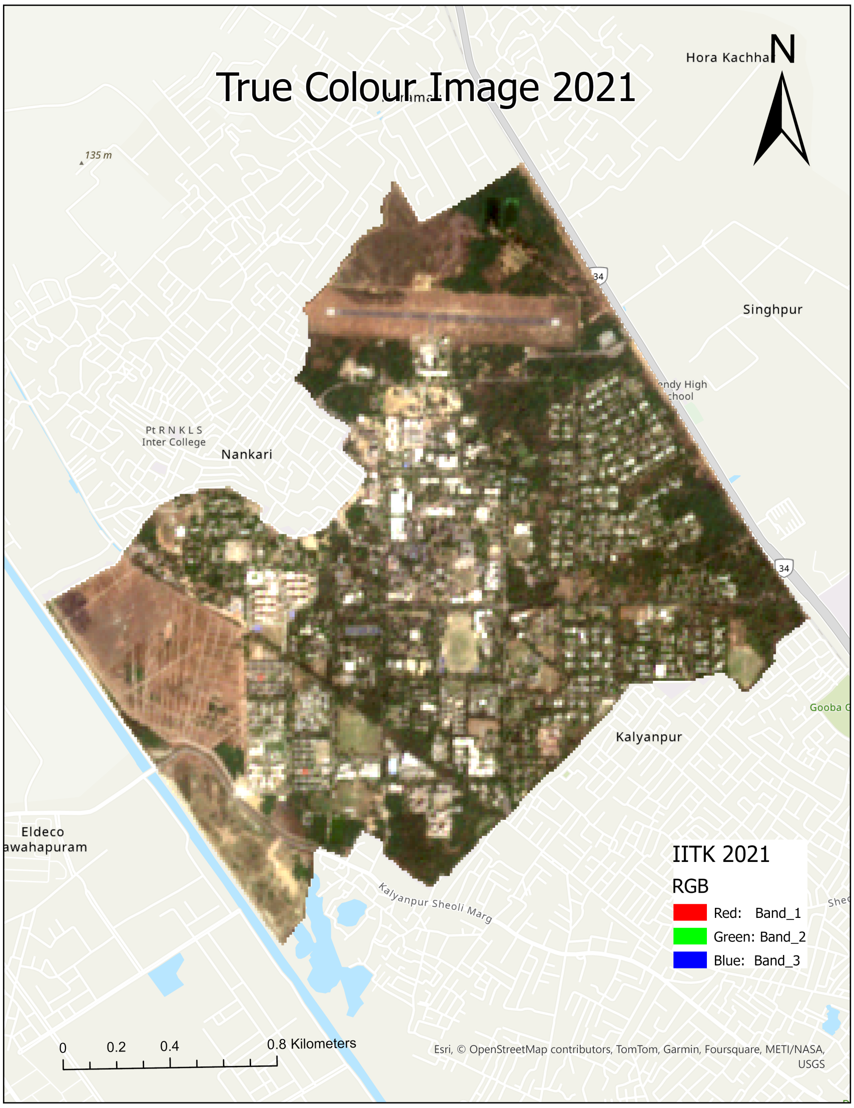

FIGURE 3.16: 2021 Sentinel-2 image

Field: Add Calculate Selection: Select By Attributes Zoom To Switch

	OBJECTID *	ClassValue	C_1	C_2	C_3	C_4	Total	U_Accuracy	Kappa
1	1	C_1	7	0	0	0	7	1	0
2	2	C_2	2	7	0	1	10	0.7	0
3	3	C_3	1	0	5	1	7	0.714286	0
4	4	C_4	5	0	0	2	7	0.285714	0
5	5	Total	15	7	5	4	31	0	0
6	6	P_Accuracy	0.466667	1	1	0.5	0	0.677419	0
7	7	Kappa	0	0	0	0	0	0	0.571231
	Click to add new row.								

FIGURE 3.18: 2021 confusion matrix

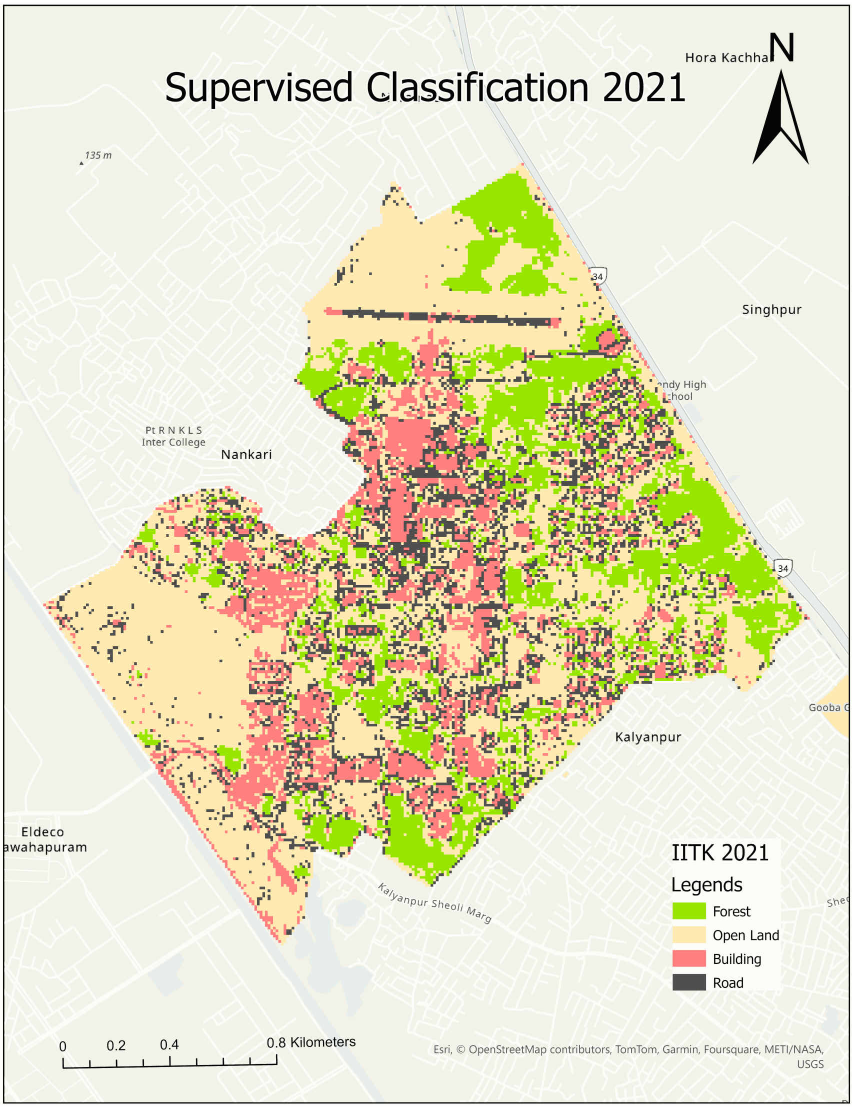

FIGURE 3.17: 2021 classified image

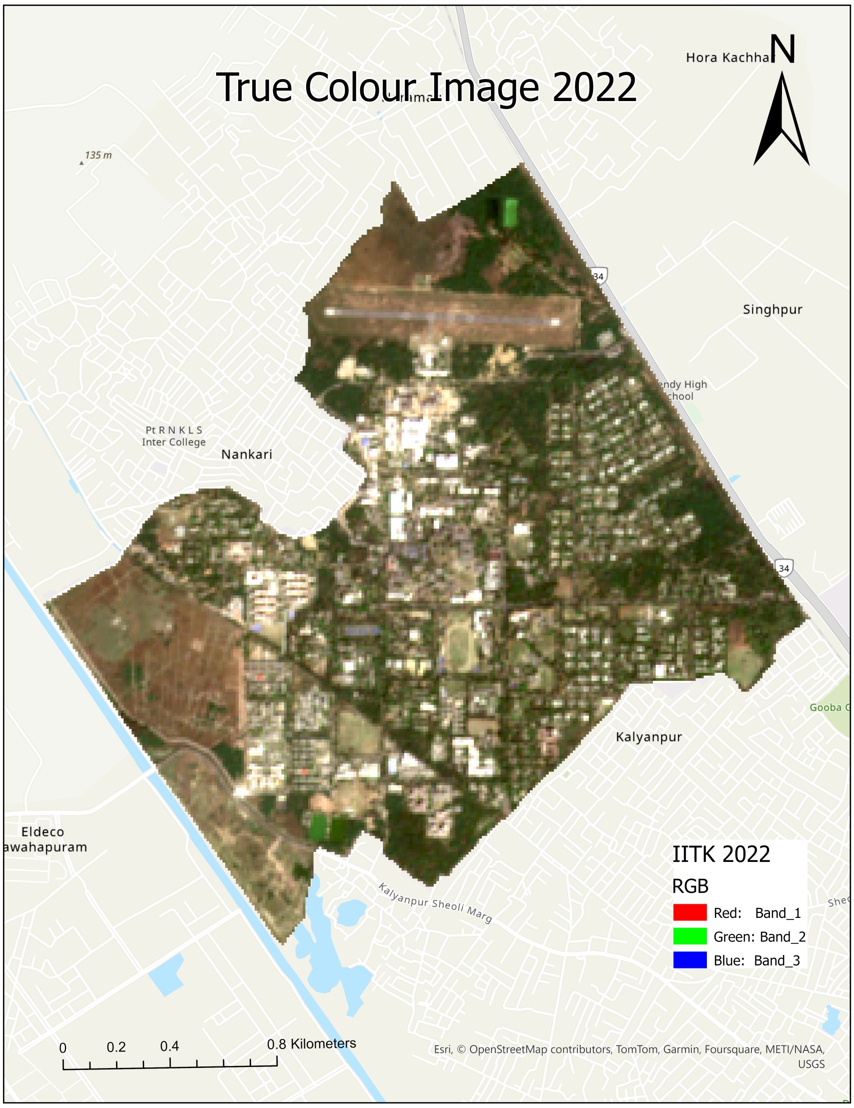

FIGURE 3.19: 2022 Sentinel-2 image

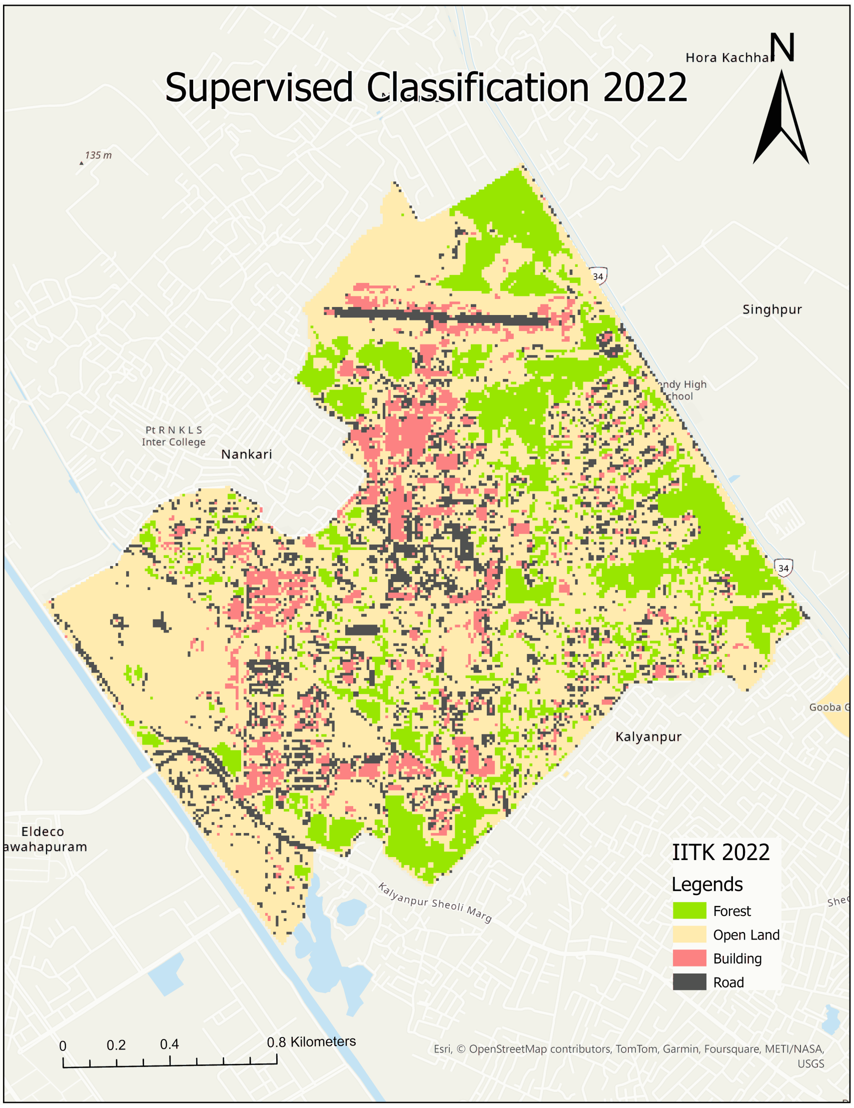

FIGURE 3.20: 2022 classified image

	OBJECTID *	ClassValue	C_1	C_2	C_3	C_4	Total	U_Accuracy	Kappa
1	1	C_1	9	0	0	1	10	0.9	0
2	2	C_2	2	10	0	0	12	0.833333	0
3	3	C_3	0	1	9	0	10	0.9	0
4	4	C_4	0	2	2	6	10	0.6	0
5	5	Total	11	13	11	7	42	0	0
6	6	P_Accuracy	0.818182	0.769231	0.818182	0.857143	0	0.809524	0
7	7	Kappa	0	0	0	0	0	0	0.745068

FIGURE 3.21: 2022 confusion image

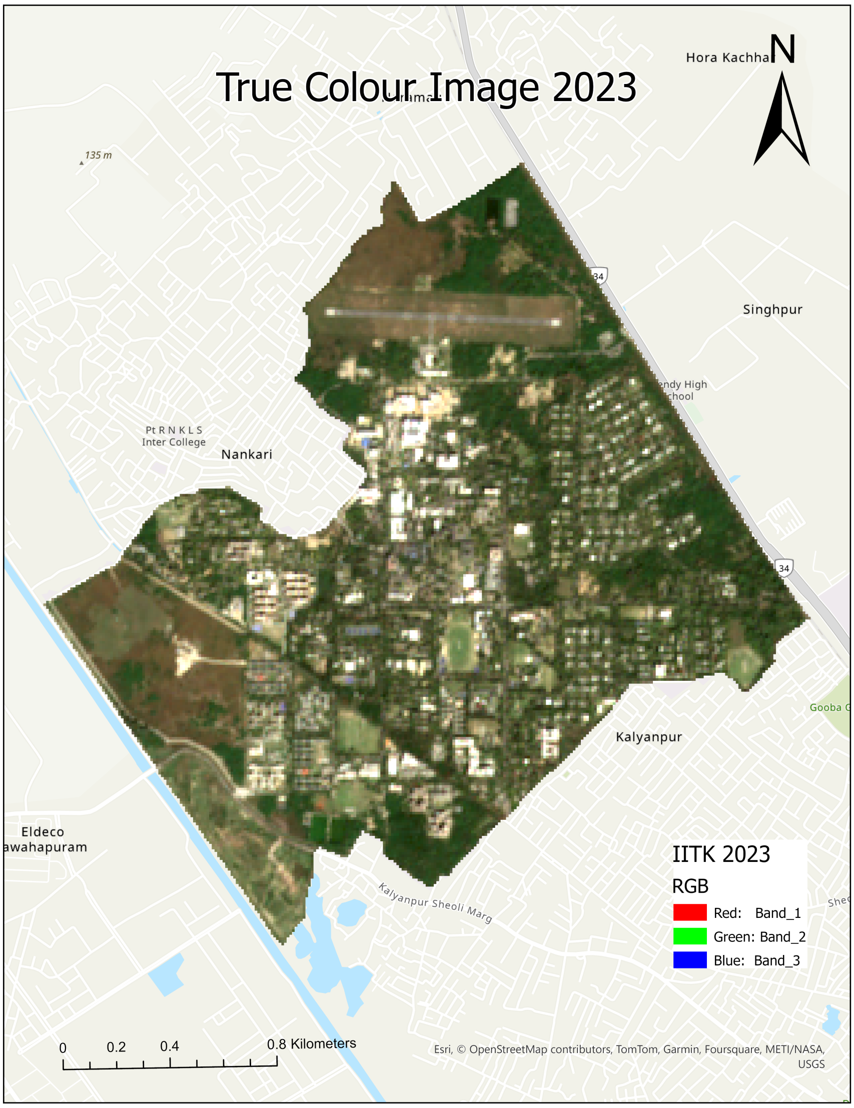

FIGURE 3.22: 2023 Sentinel-2 image

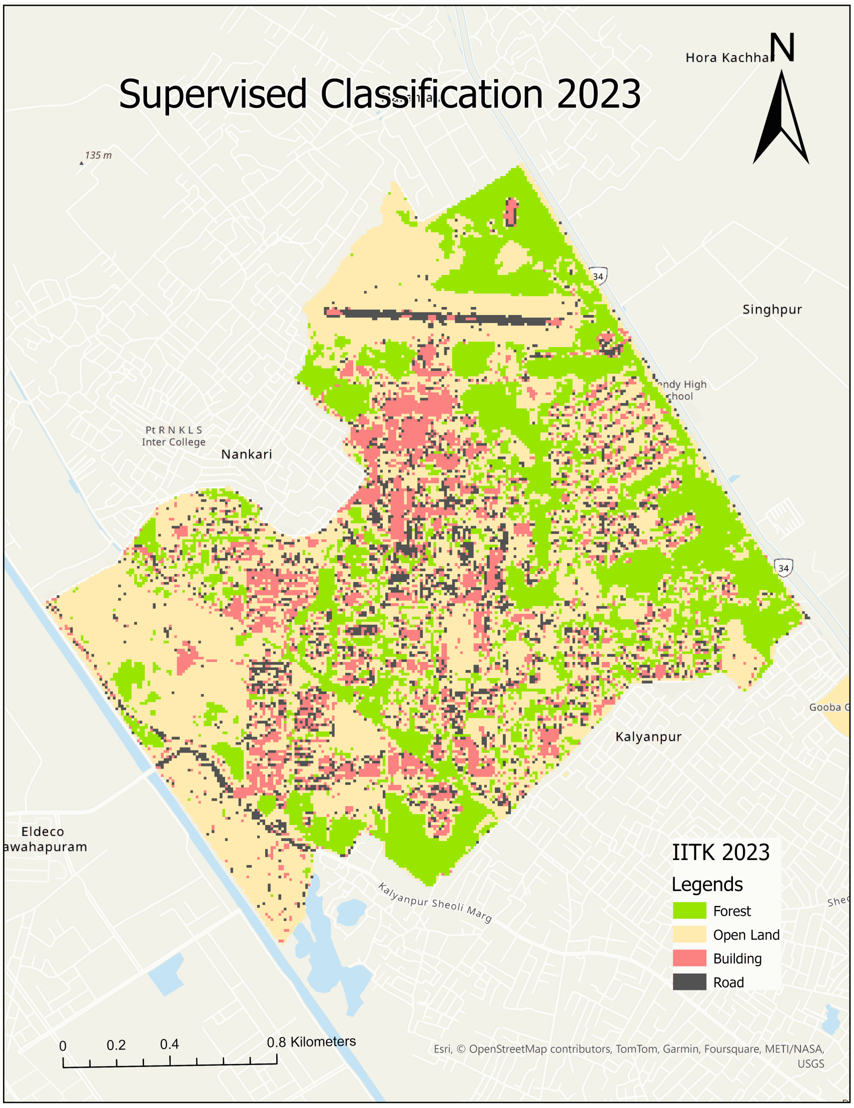

FIGURE 3.23: 2023 classified image

	OBJECTID *	ClassValue	C_1	C_2	C_3	C_4	Total	U_Accuracy	Kappa
1	1	C_1	9	0	0	1	10	0.9	0
2	2	C_2	1	7	1	1	10	0.7	0
3	3	C_3	1	0	9	0	10	0.9	0
4	4	C_4	1	1	2	6	10	0.6	0
5	5	Total	12	8	12	8	40	0	0
6	6	P_Accuracy	0.75	0.875	0.75	0.75	0	0.775	0
7	7	Kappa	0	0	0	0	0	0	0.7
	Click to add new row.								

FIGURE 3.24: 2023 confusion matrix

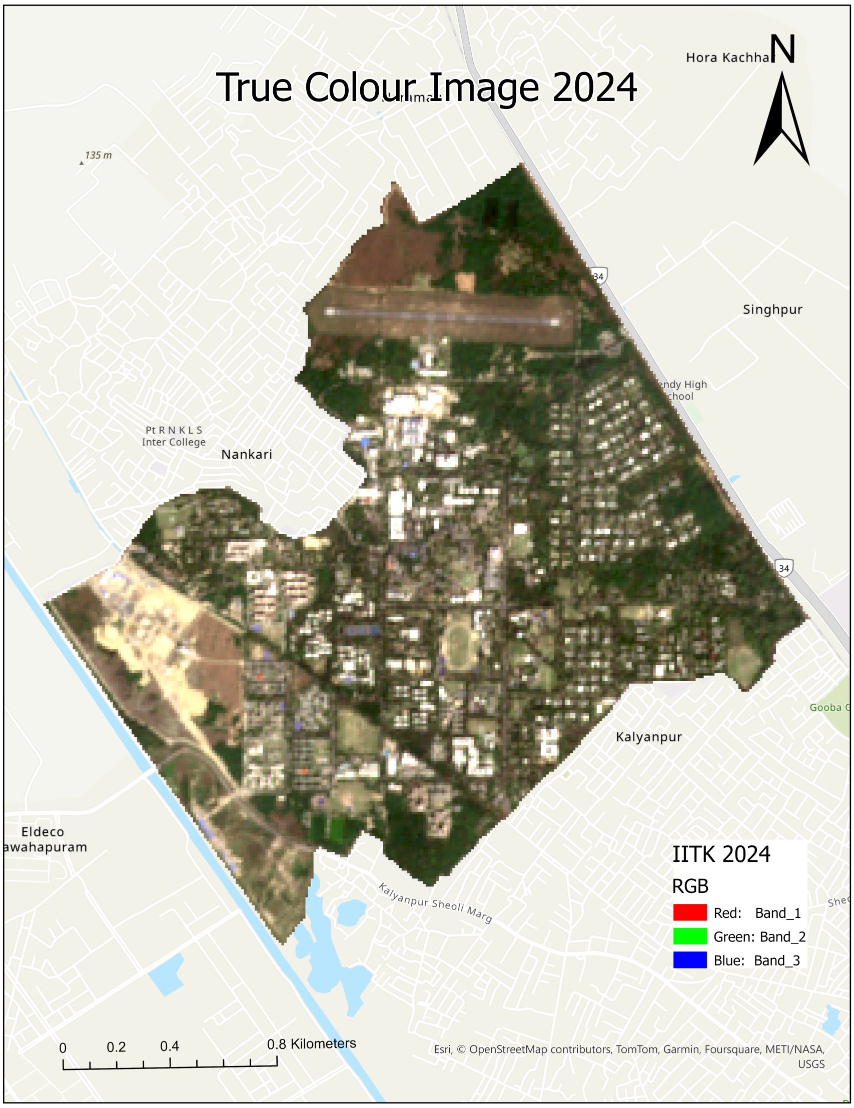

Figure 3.25: 2024 Sentinel-2 image

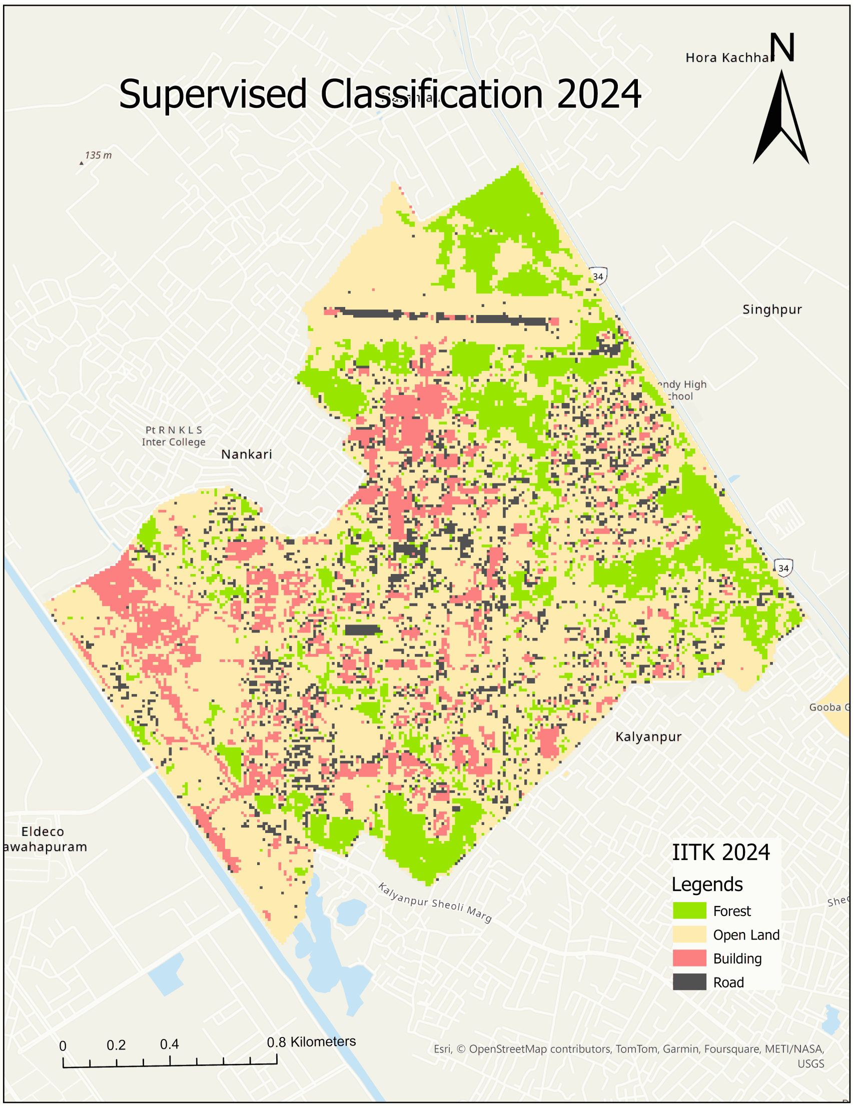

FIGURE 3.26: 2024 classified image

	OBJECTID *	ClassValue	C_1	C_2	C_3	C_4	Total	U_Accuracy	Kappa
1	1	C_1	10	0	0	0	10	1	0
2	2	C_2	2	10	0	0	12	0.833333	0
3	3	C_3	0	1	8	1	10	0.8	0
4	4	C_4	0	1	2	7	10	0.7	0
5	5	Total	12	12	10	8	42	0	0
6	6	P_Accuracy	0.833333	0.833333	0.8	0.875	0	0.833333	0
7	7	Kappa	0	0	0	0	0	0	0.777273

FIGURE 3.27: 2024 confusion matrix

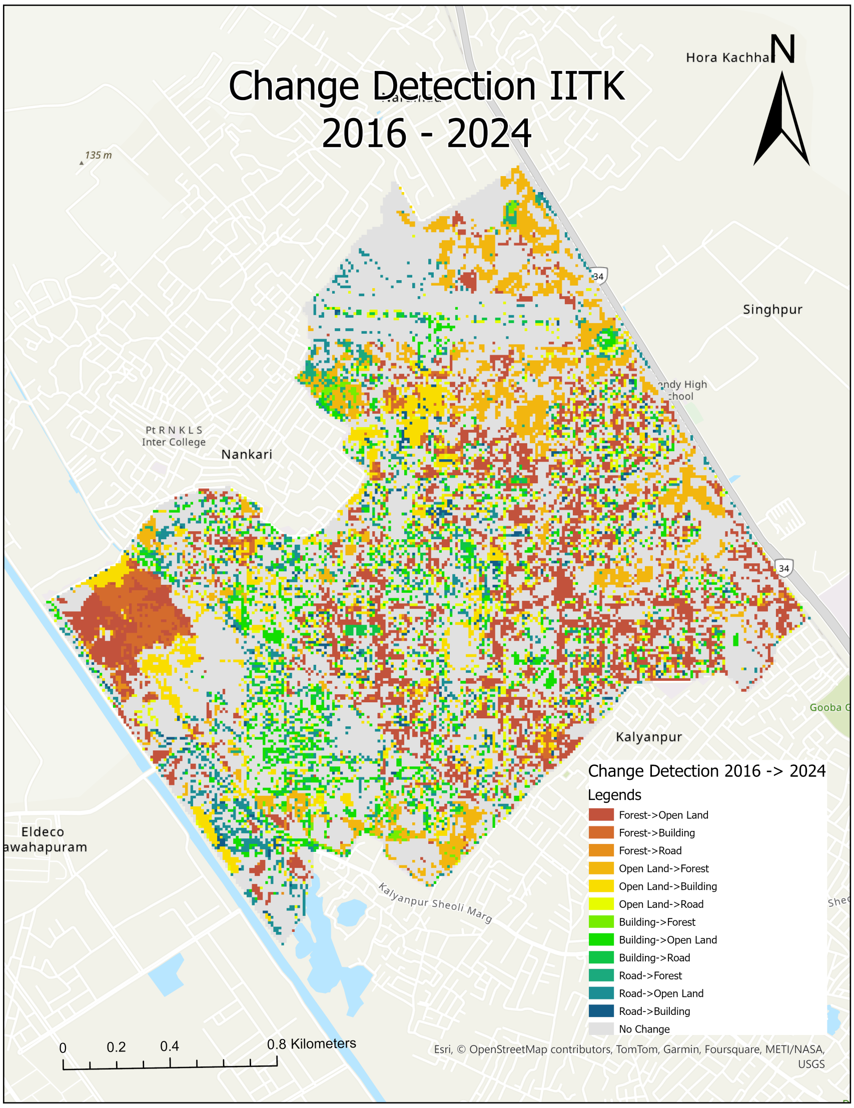

FIGURE 3.28: Change Detection from 2016 to 2024

3.2 Discussion

During our analysis of the training sample, we identified a distinct pattern among land-cover types and how it impacted the accuracy of classification. Forest pixels were relatively unique in that their spectral characteristics were more consistent than those of other classes, thus making differentiation straightforward. As a result, the forested areas were classified fairly accurately.

Open areas posed a different scenario altogether as some of the pixels for open areas were

unique, though others were mixed up with bare land and green parks. This heterogeneity led to lower classification accuracy for open areas than for forest areas.
Brightness: sometimes the pixels from buildings were overlapped by other bright surfaces in newly constructed roads or construction zones. The overlapping caused some misclassification errors with buildings since the spectral properties of the classes' pixels were similar. Finally, road pixels were very dark, often close to black, and were often inextricably mixed with the rooftops of older buildings. Since the image resolution was 10 meters, several road widths were less than one pixel wide and were frequently overlain by vegetation, which made their classification more challenging. Only large open areas, like the runway portion of IIT Kanpur, were correctly identified.

Chapter 4

Conclusion

Based on our analysis, the total forested area on campus has decreased by 29 %, while open land and building areas have expanded by 14% and 8%, respectively. Road area shows a 7% reduction, which may seem counterintuitive; however, this could be attributed to the growth of roadside trees, which obscure more of the road in satellite imagery. In conclusion, our supervised classification of high-resolution satellite imagery provides valuable insights into the patterns of land use and land cover (LULC) change, underscoring its utility for monitoring campus development and environmental transformation.

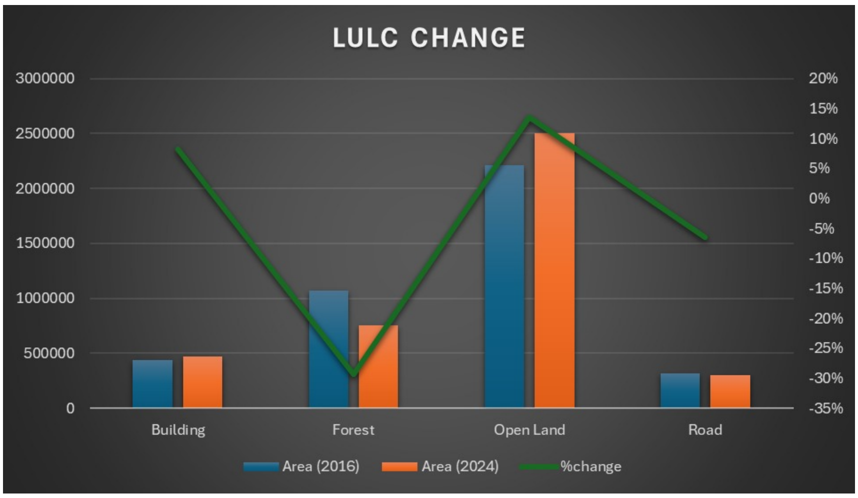

Figure 4.1: LULC change from 2016 to 2024

Bibliography

[1] Environmental Systems Research Institute (Esri), *ArcGIS Pro*, 2024. Available at: `https://www.esri.com/en-us/arcgis/products/arcgis-pro`. Accessed: 2024-11-14.

[2] European Space Agency (ESA), *Sentinel-2A User Guide*, 2024. Available at: `https://sentinels.copernicus.eu/web/sentinel/user-guides/sentinel-2-msi`. Accessed: 2024-11-14.

[3] European Space Agency (ESA), *Copernicus Open Access Hub*, 2024. Available at: `https://dataspace.copernicus.eu`. Accessed: 2024-11-14.